

# High Power Density Rectifier for Highly Efficient Future DC Distribution System

Yusuke Hayashi<sup>\*1\*2</sup>

<sup>\*1</sup>Research and Development Headquarters, NTT Facilities, Inc.  
2-13-1 Kita-otsuka, Toshima-ku, Tokyo 170-0004, Japan

<sup>\*2</sup>Division of Electrical, Electronic and Information Engineering, Graduate School of Engineering, Osaka University  
2-1 Yamada-Oka, Suita, Osaka 565-0871, Japan

<sup>\*1</sup>hayash2b@ntt-f.co.jp, <sup>\*2</sup>y\_hayashi@eei.eng.osaka-u.ac.jp

## Abstract

An approach for the high power density rectifier has been investigated to realize future highly efficient DC power distribution. The combination of ISOP (Input Series and Output Parallel)-IPOS (Input Parallel and Output Series) isolated DC-DC converter for the DC transformer and the three-phase AC-DC PWM converter using novel power devices as SiC (Silicon Carbide) transistor for the output voltage regulation has been applied. A prototype of 384 V-12 V 2.4 kW isolated DC-DC converter has been fabricated and the efficiency of 98% has been verified experimentally. The breadboard of AC 200 V-DC 384 V 2.4 kW converter has been also fabricated. The efficiency of 97% has been measured in the experiment and the potential to achieve 98% has been shown through the design consideration. The proposed methodology can be utilized for several levels of DC distribution (i.e. 12 V, 48 V, 384 V) keeping the power density and the conversion efficiency of the rectifier and contributes to the realization of highly efficient DC power distribution and future low carbonated society.

## Keywords

Rectifier; AC-DC Converter; DC-DC Converter; Input Series and Output Parallel; Input Parallel and Output Series; Silicon Carbide

## Introduction

The amount of network traffic in the data centers and the telecommunications buildings has recently been rapidly increasing due to the widespread use of information and communication technology (ICT) equipment. Energy saving in these buildings and data centers will contribute to solving some of our global environmental problems. Therefore, having a highly efficient and space-saving power supply system has become indispensable.

Since 2008, the NTT (Nippon Telegraph and Telephone) Group has been developing 380 V DC distribution system that goes beyond the conventional 48 V DC distribution system. Figure 1 shows the

configuration of the developed 380 V DC distribution system. Higher voltage reduces the current through the distribution line, and the conduction loss generated from the power converters and cables decreases. The static and the transient characteristics of the system have been evaluated, and the availability has been verified in the demonstration sites.

Now, the advanced DC distribution system has been proposed to realize future low carbonated society. The schematic diagram of the proposed system is shown in Fig. 2. The conversion efficiency has to be improved from 80% in the conventional 380 V DC distribution system to 94% in the proposed system. The high power density (highly efficient and space-saving) power converters such as the interface AC-DC converter and the isolated DC-DC converter with high voltage transformation ratio are necessary.

In this paper, the current 380 V DC distribution system and the advanced DC distribution system were introduced at first. Then, the circuit topology of the isolated DC-DC converter and the AC-DC converter were proposed to realize the total efficiency of 94% in the advanced DC distribution system. The availability of the proposed topology has been verified by fabricating the converter prototypes and the possibility to achieve the above efficiency was shown by the design consideration.

## Highly Efficient Future DC Distribution System

The schematic diagram of the current 380 V DC distribution system has been shown at first. Then, the configuration of the advanced DC distribution system has been proposed to accomplish higher efficiency. The numbers of the conversion stages and the required functions of the power converter were discussed here.

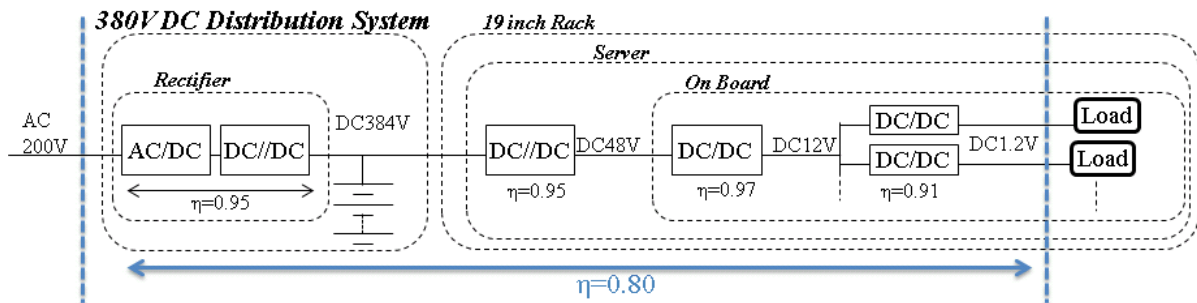


FIG 1 Schematic Diagram of 380 V DC Distribution System

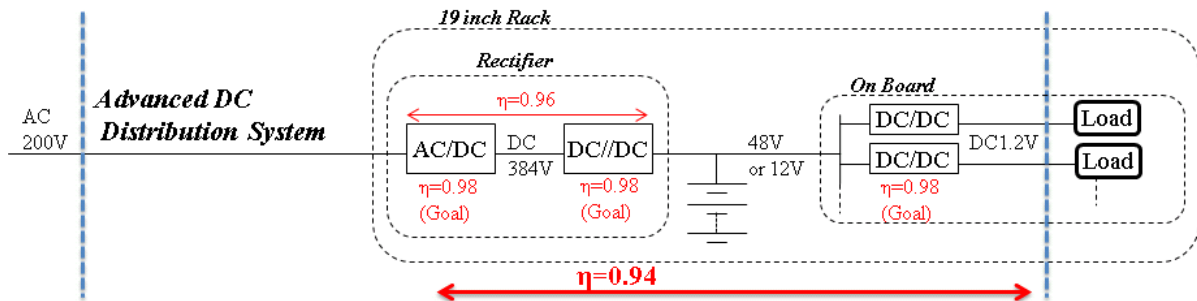


FIG 2 Schematic Diagram of Advanced DC Distribution System in 2020

### Current 380 V DC Distribution System

Figure 1 shows the schematic diagram of the current 380 V DC distribution system. This system has five conversion stages from the AC 200 V input to the DC 3.3 V or 1.2 V loads and total conversion efficiency is 80 %. Details are as follows:

- A rectifier for DC 380 V distribution system has two stages: the AC-DC converter as the PFC (power factor correction) and the isolated DC-DC converter for the output voltage regulation. The efficiency of the 200 V-384 V rectifier is 95%.
- The PSU (power supply unit) is installed as the front-end converter into ICT (Information and Communication Technology) equipment such as servers. The efficiency of the 384 V-48 V is 95%.
- The step-down on-board converters are installed into the ICT equipment as POL (Point of Load) converters. The efficiencies of the 48 V-12 V and 12 V-3.3 V are 97 % and 91 % respectively.

The conversion efficiency 95 % is the experimental result of the current 380 V DC power supply. The efficiencies of the DC-DC converters in ICT equipment are based on the published datasheets. To achieve 94% in the 380 V DC distribution system, the

efficiency of 98.8 % is required for the power converter in each stage. In terms of the DC 380 V rectifier, the conversion efficiency has to be improved from 95% to 97.6%. The higher performance semiconductor power devices and magnetic core materials are indispensable to accomplish the above conversion efficiency in case that the number of conversion stages and the converter functions are conventional.

### Advanced DC Distribution System

Figure 2 shows the schematic diagram to achieve total efficiency of 94% from the AC 200 V input to the DC 3.3 V or 1.2 V loads. This consists of three conversion stages. The characteristics of the converters are summarized as follows:

- The AC-DC converter is installed for the AC interface and the DC output voltage control. Three-phase PWM converter based on the classical control theory using novel power devices is one of solutions.
- The highly step-down isolated DC-DC converter is necessary for the voltage transformation and the galvanic isolation. The solid state transformer without the output voltage regulation is available because the input voltage is controlled by the AC-DC converter in the primary side.
- The non-isolated DC-DC converter as POL is

installed for the load voltage regulation

In each stage, the conversion efficiency of 98% has to be accomplished to realize the total efficiency 94%. For the rectifier in the advanced DC distribution, the efficiency of 96% is required. The details of the AC-DC converter and the isolated DC-DC converter to achieve the efficiency of 96% are shown in the next chapter.

### Development of High Power Density Rectifier for Advanced DC Distribution

The circuit topology is introduced to realize the highly efficient 96% rectifier in the advanced DC distribution system. Two power converters in Fig. 2 are emphasized. One is the high step-down ratio DC transformer based on the ISOP-IPOS topology and the other is the general three-phase AC-DC converter using SiC power devices. Details are shown in this chapter.

#### DC-DC Converter Based on ISOP-IPOS Topology

Multi-converter approach proposed to apply the on-board power supply technology for the advanced DC distribution system is based on the ISOP (Input Series and Output Parallel) and IPOS (Input Parallel and Output Series) connection topology of modular power converters, in which the conversion efficiency and the power density of the designated converter are determined by the performance of single modular converter. It is expected that the high power density isolated DC-DC converter is developed simply by using highly integrated low voltage converter modules.

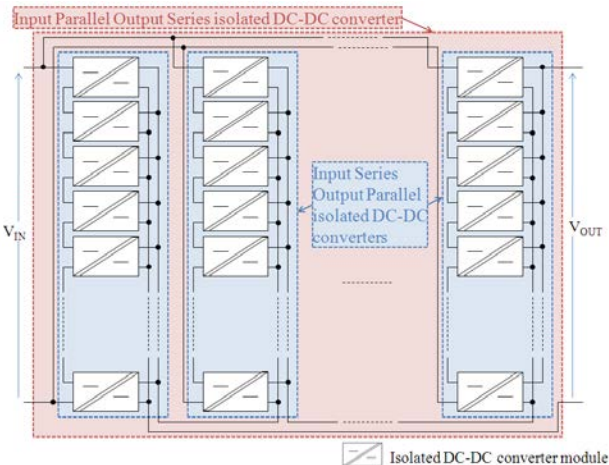


FIG 3 SCHEMATIC DIAGRAM OF ISOLATED DC-DC CONVERTER BASED ON ISOP-IPOS TOPOLOGY

Figure 3 shows the schematic diagram of an isolated converter based on the ISOP and IPOS connection

topology. Characteristics are summarized as follows:

- The ISOP topology is applied to reduce the input voltage stress of each modular isolated DC-DC converter. To balance the input voltage, the output terminal of each converter is connected in parallel.
- To realize high output voltage, the IPOS topology is applied to several ISOP converters. The output voltage in each ISOP converter depends on the commonly connected input voltage and counterbalances because the output current in each ISOP converter is equal.

By considering the above topology, the commercially available high power density converter for on-board power supply is available to fabricate the DC transformer simply. Generally, the power density of the low voltage converters tends to be higher than that of the high voltage converters and the low voltage on-board converter with several tens of  $W/cm^3$  is now available. The design considerations for not only a SiC high voltage converter but also a GaN low voltage converter are of essential importance in realizing a high power density DC transformer.

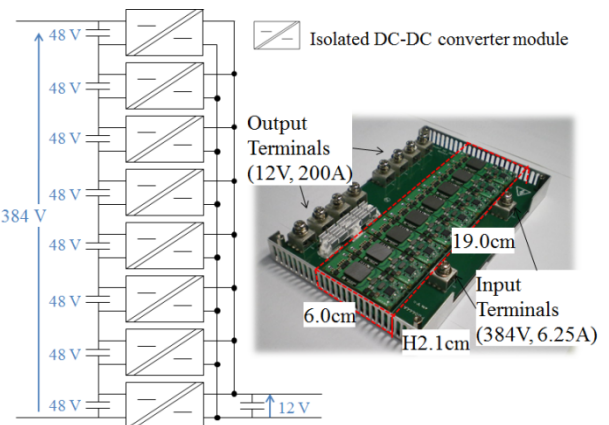


FIG 4 CIRCUIT CONFIGURATION AND OVERVIEW OF FABRICATED 384 V-12 V 2.4 KW DC-DC CONVERTER

The 384 V-12 V isolated converter can be developed by using 48 V-12 V converters based on the ISOP topology. Utilization of the 48 V-12 V isolated converters with the efficiency of 98% (VICOR: IB048E120T40N1-00) is attractive to fabricate the designated converter with high efficiency and ultra compact. Figure 4 shows the photograph of the fabricated DC-DC converter and the conversion efficiency supported by VICOR Japan is shown in Fig. 5. The converter volume is  $239.1 \text{ cm}^3$  ( $= 6.0 \text{ cm} \times 19 \text{ cm} \times 2.1 \text{ cm}$ ) and the power density is  $10 \text{ W/cm}^3$  ( $= 2400 \text{ W} / 239.1 \text{ cm}^3$ ). Here, the volume of the auxiliary circuits is considered and the volumes caused by the terminals

and the fan for the forced air cooling are not taken into account.

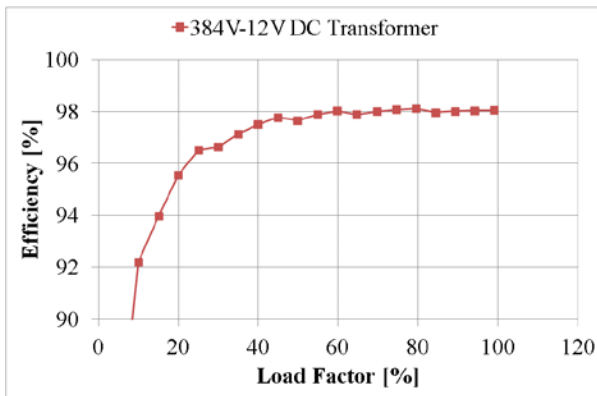


FIG. 5 CONVERSION EFFICIENCY OF 384 V-12 V 2.4 KW DC TRANSFORMER USING 48V-12V CONVERTERS

In the ISOP and IPOS topology, the rectifiers with the output voltage of 48V and 384 V can be realized keeping the conversion efficiency of 98% and the power density of 10 W/cm<sup>3</sup> because these performances are based on single modular DC-DC converter. This topology is available not only for the rectifier in the advanced DC distribution but also the one in the current 380 V DC distribution system. The number of installed modular converters increases and contributes to reducing the converter cost and realizing the widespread use of power electronics converters in the future.

#### AC-DC Converter Using SiC Power Devices

To utilize the DC transformer in the advanced DC distribution system, the input voltage of the DC transformer has to be controlled at a constant value by the AC-DC converter at the primary side. The PFC converter based on the single-phase circuit topology has been applied for the rectifier in the current 380 V DC distribution system. Issues are summarized as follows:

- The output DC voltage of the PFC is not controlled at a constant value.
- The large capacitance is required for the output smoothing capacitor to compensate the power fluctuation caused by the twice of the fundamental frequency.

The general 3-phase hard-switching PWM topology is one of solutions for the above issues. The output DC voltage can be regulated by the classical control and the output capacitance can be reduced by increasing switching frequency. This has the potential to achieve high power density of the 200 V-384 V converter.

There are two key issues for creating a high power

density 3-phase PWM converter. One is the use of ultra-low loss semiconductor power devices to downsize the heat sink volume. The other is the high frequency operations to minimize the volume of the passive components. A full SiC combination such as the SiC-JFET and the SiC-SBD pair would allow for the ideal behavior necessary for the PWM converter. Synchronous rectification is useful for decreasing the conduction loss of the SiC-SBD, because the SiC-JFET has low resistance without body diode.

TABLE1 PARAMETERS FOR 384V-12V DC TRANSFORMER

|                   |  |
|-------------------|--|
| Output Power      | 2400 W                                     |
| Input Voltage     | 384 V                                      |
| Output Voltage    | 12 V                                       |
| Efficiency        | 98%<br>(from 60% to 100% load)             |
| Modular Converter | IB048E120T40N1-00<br>(VICOR: 48V-12V, 98%) |

TABLE2 PARAMETERS FOR EXPERIMENT

|                                     |  |
|-------------------------------------|--|
| Circuit Configuration               | Six-Switch Full Bridge AC-DC Converter |
| Output Power P <sub>OUT</sub>       | 2400 W                                 |
| Input Voltage V <sub>IN</sub>       | AC 200 V                               |
| Output Voltage V <sub>OUT</sub>     | DC 384 V                               |
| Switching Frequency f <sub>sw</sub> | 50 kHz                                 |
| Main Switch                         | SiC-JFET<br>(Semisouth: 1200 V, 63 mΩ) |
| Free-Wheeling Diode                 | SiC-SBD<br>(SiCED: 1200 V, 5 A)        |
| Input Inductor                      | 1000 μH per phase                      |
| Output Capacitor                    | 66 μF                                  |
| Digital Controller                  | TMS320C6713<br>(Myway: PE-Expert III)  |

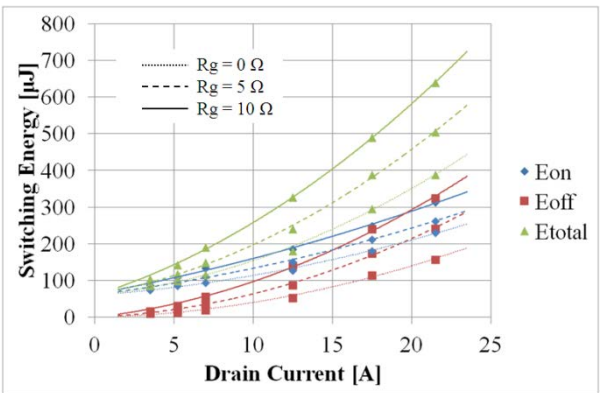


FIG. 6 SWITCHING LOSS ENERGY OF SiC-JFET AND SiC-SBD COMBINATION IN DOUBLE-PULSE TEST CIRCUIT

Table 2 shows the parameters for the demonstration of the SiC AC-DC converter. The 1200 V SiC-JFET from Semisouth and the 1200 V SiC-SBD from SiCED are employed here. Switching loss energy of the SiC-JFET and the SiC-SBD combination has been measured and the measurement results are shown in Fig. 6. The turn-on and turn-off switching energies are shown

here when the external gate resistance  $R_g$  is varied from  $0 \Omega$  to  $10 \Omega$ . The inductance of the single-phase AC inductor and the capacitance of the DC capacitor are  $1000 \mu\text{H}$  and  $66 \mu\text{F}$ , respectively.

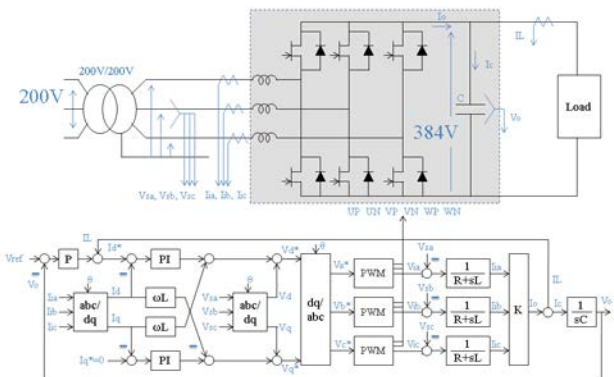


FIG 7 CIRCUIT CONFIGURATION AND CONTROL DIAGRAM OF AC-DC CONVERTER

Figure 7 shows the circuit configuration and the block diagram of the control system for the SiC AC-DC converter. The general PWM control is applied and the gate signals are generated by using the digital controller PE-Expert III from Myway. Figure 8 shows the fabricated prototype of the converter. The total volume of the converter is  $1170 \text{ cm}^3$  ( $= 12.5 \text{ cm} * 19.0 \text{ cm} * 5.0 \text{ cm}$ ) and the power density is  $2.0 \text{ W/cm}^3$ . The full bridge circuit boards with SiC power devices, the gate drivers, the input inductors, the output capacitors and the heat sinks without the forced air cooling fan have been considered to estimate the volume.

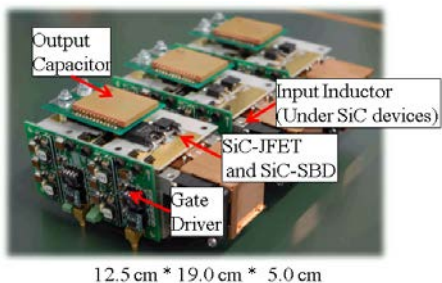


FIG. 8 OVERVIEW OF SiC AC-DC CONVERTER PROTOTYPE

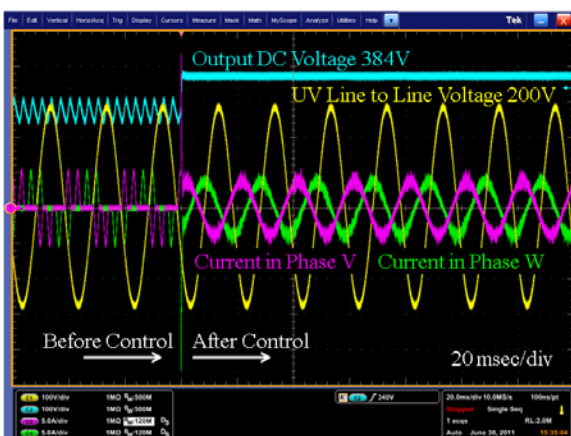


FIG 9 STEADY STATE WAVEFORM IN PWM CONVERTER

The steady state waveform in the experiment is shown in Fig. 9. The line to line input voltage between the phase U and the phase V, the output DC voltage and input currents in phases V and W are shown here. After PWM control, the input currents are sinusoidal and the output DC voltage is controlled at 384 V.

Figure 10 shows the converter power loss and the conversion efficiency of the fabricated AC-DC converter. Total converter loss was measured by using the power meter (WT3000: Yokogawa). Maximum conversion efficiency is 97.0% at the half load and the efficiency at the full load is 96.0%. To realize the high power density rectifier for the advanced DC distribution system, the maximum efficiency of 98% is necessary for the AC-DC converter. The approach to achieve the efficiency is discussed by the design consideration in the next chapter.

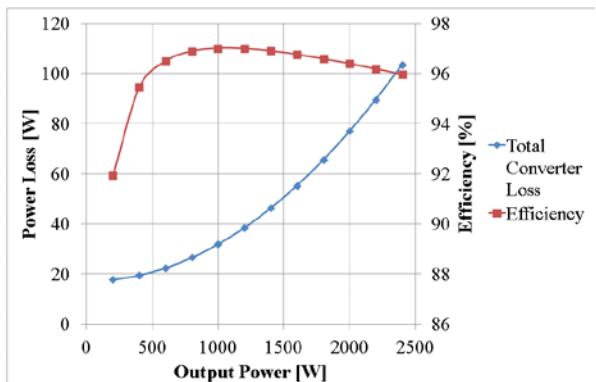


FIG. 10 CONVERTER POWER LOSS AND CONVERSION EFFICIENCY OF SiC AC-DC CONVERTER

## Design Consideration for 3-phase PWM Converter using SiC JFETs and SiC-SBDs

### High Power Density Design Methodology

An integrated power converter design tool has been developed to estimate converter power density and components' volumes under high-speed and high-frequency switching operation. A design flowchart is shown in Fig. 11 and the features are summarized as follows:

- A power loss limit model is applied to estimate the switching loss energy generated from unipolar power devices. In high-speed hard switching operations, the switching energy is described by the total amount of the stored energies caused by the device junction capacitance and the circuit parasitic parameters.
- A core loss calculation method using a loss map is employed. The loss map is the database of core loss energies related to the dynamic

minor loop's area under the real PWM operation.

- The optimization process such as the downhill simplex method is conducted by using ISIGHT software. The optimal parameters for maximizing the power density or the efficiency are extracted, taking the structure design and the thermal design into account.

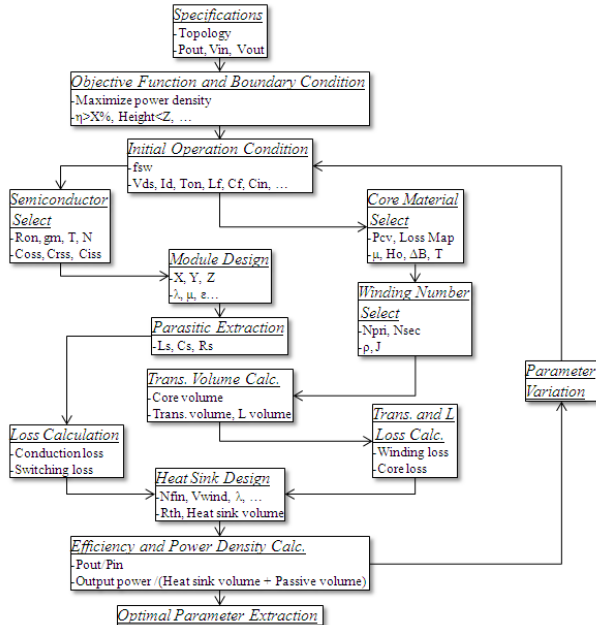


FIG. 11 DESIGN FLOWCHART FOR HIGH POWER DENSITY CONVERTER

By means of the above methods, the converter power loss is exactly estimated. The power density of the AC-DC converter is calculated by estimating the volume of the heat sink, taking the power loss into account. Following equations are utilized to calculate the power density.

$$PD = \frac{P_{OUT}}{V_{CONV}} \quad (1)$$

$$V_{CONV} = V_{CB} + V_{GD} + V_L + V_C + V_{HS} (P_{JFET} \cdot P_L) \quad (2)$$

The  $PD$  in Eq. (1) represents the power density of the converter.  $V_{CONV}$  and  $P_{OUT}$  are the converter volume and the converter output power, respectively. The converter volume  $V_{CONV}$  consists of the volume of the circuit board with power devices  $V_{CB}$ , the volume of the gate drivers  $V_{GD}$ , the input inductor volume  $V_L$ , the output capacitor volume  $V_C$ , and the heat sink volume  $V_{HS}$  mainly.

The power loss generated from a SiC-JFET  $P_{JFET}$  consists of the conduction loss  $P_{COND}$  and the switching loss  $P_{SW}$ . The approximation formula shown in Eq. (4) is available to calculate the conduction loss  $P_{COND}$ . In

Eq. (4),  $V_{TH}$  and  $R_{ON}$  are the threshold voltage and the on-resistance of the power device, respectively.  $I_M$ ,  $m_a$ , and  $\phi$  are the peak current through the device, the amplitude modulation factor and the power factor, respectively.

$$P_{JFET} = P_{COND} + P_{SW} = P_{COND} + f_{SW} \cdot E_{SW} \quad (3)$$

$$P_{COND} = V_{TH} \cdot I_M \left( \frac{1}{\pi} \pm \frac{m_a}{4} \cos \phi \right) \quad (4)$$

$$+ R_{ON} \cdot I_M^2 \left( \frac{1}{4} \pm \frac{2m_a}{3\pi} \cos \phi \right)$$

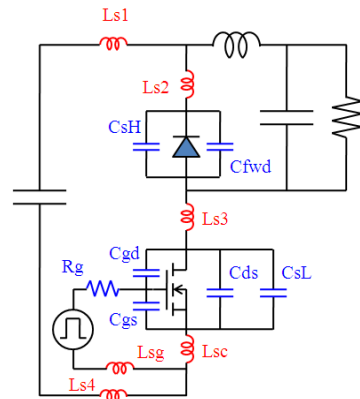


FIG. 12 EQUIVALENT CIRCUIT FOR SWITCHING ENERGY ESTIMATION IN HIGH-SPEED HARD SWITCHING OPERATION

Figure 12 shows the equivalent circuit to estimate the switching energy in the high-speed hard-switching operation. The switching loss is calculated as shown in Eq. (5) based on the power loss limit model.

$$E_{SW} = E_{on-t} + E_{off-t} + E_{oss} + E_{FWD} + E_{Ls} + E_{Cs} \quad (5)$$

$$\geq E_{oss} + E_{diode} + E_{Ls} + E_{Cs}$$

Where,  $E_{on-t}$  and  $E_{off-t}$  are the time-dependent switching energies affected by the gate resistance  $R_g$ .  $E_{oss}$  is the stored energy in the output capacitance of the SiC-JFET, and  $E_{FWD}$  is the stored energy in the junction capacitance of the SiC-SBD.  $E_{Cs}$  and  $E_{Ls}$  are the stored energies in the parasitic capacitance and the parasitic inductance of the circuit board. Time-dependent switching loss energies are negligible in high-speed switching operation and the minimum switching loss energy is described as the total amount of the stored energies.

The power loss from the inductor  $P_L$  consists of the copper loss  $P_{Cu}$  and the core loss  $P_{CORE}$ . The following equations Eq. (6) to Eq. (10) are used to estimate the core loss and the core volume of the inductor.

$$P_L = P_{Cu} + P_{CORE} = P_{Cu} + \sum_{f_{sw}} E_{CORE} \quad (6)$$

$$E_{CORE} = f(H_O, \Delta B, f_{sw}, V_{CORE}) \quad (7)$$

$$H_O = \frac{N_i L}{l_e} \quad (8)$$

$$\Delta B = \frac{\Delta \phi}{S_e} = \frac{1}{N S_e} \int v_L dt \quad (9)$$

$$V_{core} = S_e \times l_e \quad (10)$$

Where,  $N$ ,  $S_e$ , and  $l_e$  correspond to the turn number of the winding, the effective magnetic length and the effective cross sectional area of the magnetic core respectively. The induced voltage and the current of the inductor are  $v_L$  and  $i_L$  respectively. The core volume of the inductor  $V_{core}$  is calculated using  $S_e$  and  $l_e$ . The core loss energy of the inductor  $E_{core}$  is determined by the bias magnetic field  $H_O$ , the magnetic flux density  $\Delta B$ , the core volume  $V_{core}$ , and the loss map database. Figure 13 shows the loss map database of the magnetic core material utilized in the experiment. The core loss energies are plotted on the map taking the PWM switching operation into account and the core loss  $P_{core}$  is calculated by accumulating the plotted energies.

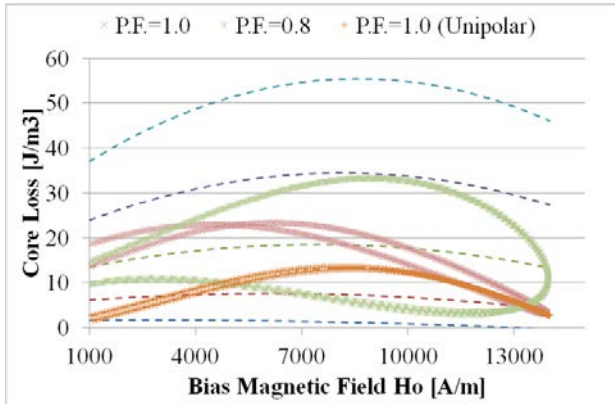


FIG. 13 LOSS MAP OF MAGNETIC CORE MATERIAL AND CORE LOSS TRAJECTORY IN INVERTER PWM OPERATION

#### Design Consideration For Highly Efficient 98% AC-DC Converter

Design consideration for 2.4 kW AC 200 V to DC 384 V converter is carried out to achieve the efficiency of 98% needed to the rectifier for the advanced DC distribution. In this section, the potential of the SiC power device for higher efficiency is discussed, taking device intrinsic parameters into account.

The circuit configuration is shown in Fig. 14 and the parameters for the design is shown in Table 3. Device parameters of the SiC-JFET (Semisouth: 1200 V, 63 mΩ) and the SiC-SBD (SiCED: 1200 V, 5 A) have been extracted and the magnetic core material utilized in the experiment was assumed here. The detailed characteristics of the SiC-JFET is shown in Fig. 15.

Design parameters as the switching frequency, the current density and the gate resistance were varied to maximize the converter power density. The design parameters for passive components are fixed to evaluate the potential of the SiC power devices here.

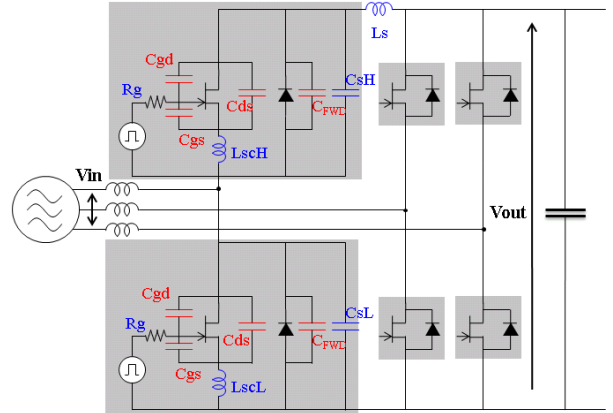


FIG. 14 CIRCUIT CONFIGURATION OF THREE-PHASE AC-DC CONVERTER DESIGN

TABLE3 PARAMETERS FOR AC-DC CONVERTER DESIGN

| Concerter Circuit                |  |
|----------------------------------|--|
| Circuit Topology                 | Six-Switch Full Bridge AC-DC Converter |
| Output Power $P_{out}$           | 2400 W                                 |
| Input Voltage $V_{in}$           | AC 200 V                               |
| Output Voltage $V_{out}$         | DC 384 V                               |
| Power Devices                    |  |
| Main Switch                      | SiC-JFET(1200 V, 63 mΩ)                |
| Free-Wheeling Diode              | SiC-SBD(1200 V, 5 A)                   |
| Switching Frequency $f_{sw}$     | 50 kHz to 200 kHz                      |
| Current Density $J$              | 50 A/cm² to 400 A/cm²                  |
| Gate resistance $R_g$            | 0 Ω to 10 Ω                            |
| Parasitic Inductance $L_s$       | 0 nH to 50 nH                          |
| Parasitic Capacitance $C_s$      | 0 pF to 100 pF                         |
| Input Inductor                   |  |
| Permeability $\mu_r$             | 64                                     |
| Bias magnetic field $H_O$        | 5000 A/m                               |
| Magnetic flux Density $\Delta B$ | 0.2 T (Maximum)                        |

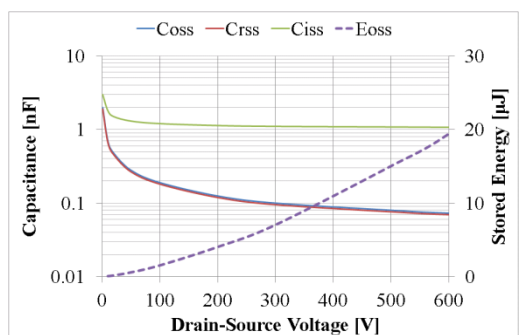


FIG. 15 CV CHARACTERISTICS OF SiC-JFET AND STORED ENERGY IN OUTPUT CAPACITANCE

Figure 16 shows the calculation results of the converter power loss and the efficiency when the switching frequency varies from 10 to 200 kHz. Here,

the gate resistance and the current density of the SiC-JFET are  $5.0\ \Omega$  and  $50\ A/cm^2$  respectively. The circuit parasitic inductance is  $36\ nH$ , the low side parasitic capacitance is  $40\ pF$  and the high side parasitic capacitance is  $10\ pF$ . These are based on the condition in the experiment.

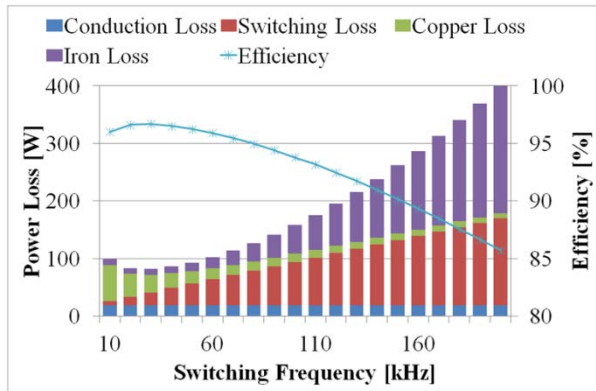


FIG. 16 ESTIMATED CONVERTER POWER LOSS AND EFFICIENCY

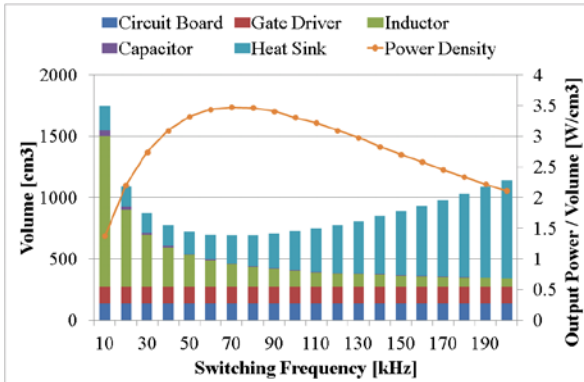


FIG. 17 ESTIMATED CONVERTER VOLUME AND POWER DENSITY

Figure 17 shows the calculation result of the converter components' volume and the power density. The circuit board including SiC-JFETs and SiC-SBDs, the gate drivers, the input inductors, the output capacitors and the heat sink were considered here. The volume of the fan for the forced air cooling and the interspace were not taken into account. The components' volumes at 50 kHz operation corresponded to the volumes in the experiment shown in Fig. 8.

The conversion efficiency is 96% at 50 kHz switching operation in Fig. 16 and this result has good agreement with the experimental result shown in Fig. 10. The maximum efficiency is 97% at 30 kHz switching operation. When the switching frequency varies from 50 kHz to 30 kHz to improve the efficiency, the power density decreases as shown in Fig. 17.

To evaluate the potential of the power devices, power loss limit model is attractive. The power loss limit

model means that the minimum switching loss energy is determined by the stored energy in the output capacitance shown in Fig. 15 when the parasitic parameters and the switching time are negligible. The improvement of the conversion efficiency and the power density is expected by the reduced switching loss.

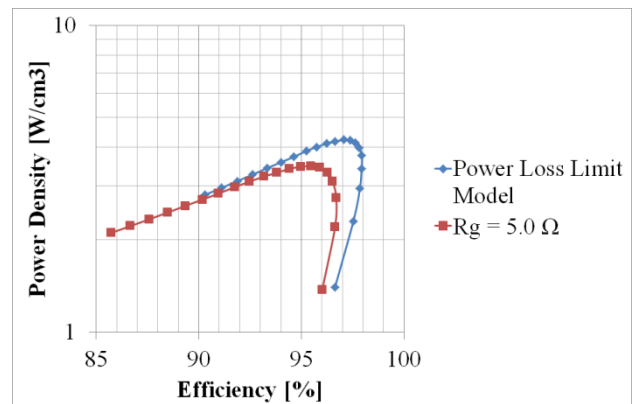


FIG. 18 ESTIMATED CONVERTER EFFICIENCY AND POWER DENSITY

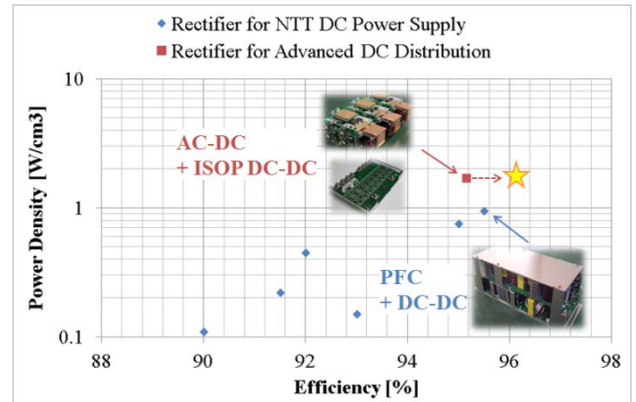


FIG. 19 POWER DENSITY TREND OF RECTIFIER FOR DC DISTRIBUTION SYSTEM

Figure 18 shows the relationship between the conversion efficiency and the power density. The red curve is drawn by using the calculation results shown in Figs. 16 and 17. The blue curve means the calculation result when the power loss limit model is applied to evaluate the potential SiC power devices. The maximum conversion efficiency is improved from 97% at 30 kHz switching operation to 98% at 50 kHz operation. The increase of the power density is also expected because of the smaller heat sink caused by the higher efficiency and the smaller passive component in higher switching frequency. By taking full advantage of the performance of the SiC power devices, highly efficient and high power density AC-DC converter will be realized.

Figure 19 shows the power density trend of the rectifier for DC distribution system. The power

density of the rectifier for the 380 V DC distribution system is now at a level of 1 W/cm<sup>3</sup> with the efficiency of 95.5%. For the proposed topology, the power density of 1.7 W/cm<sup>3</sup> with the efficiency of 95% (= 98% \* 97%) was verified experimentally and the potential to achieve 96 % (= 98 % \* 98 %) was also shown.

## Conclusions

The advanced DC distribution system was proposed for future low carbonated society. The proposed DC distribution system required total conversion efficiency of 96% for the rectifier, in which highly efficient 98% power converters were necessary. The DC transformer based on ISOP-IPOS topology and the PWM AC-DC converter using SiC power devices were proposed for the highly efficient rectifier.

The prototype of the DC transformer (384 V to 12 V, 2.4 kW, 10 W/cm<sup>3</sup>) was developed and the efficiency of 98 % was verified in the experiment.

The prototype of the AC-DC converter (200 V to 384 V, 2.4 kW, 2 W/cm<sup>3</sup>) using SiC-JFET and SiC-SBD was fabricated and the maximum efficiency of 97% was confirmed experimentally. The approach for 98% efficiency was shown by the design consideration.

The proposed methodology can be utilized for several levels of DC distribution (i.e. 12 V, 48 V, 384 V) keeping the power density and the conversion efficiency of the rectifier and contributes to realizing highly efficient DC power distribution and future low carbonated society.

## REFERENCES

Aggeler, D., Biela, J. and Kolar, J. W.. "A compact, high voltage 25kW, 50 kHz DC-DC converter based on SiC JFETs." in: Proceedings of 23rd Annual IEEE Applied Power Electronics Conference and Exposition (APEC), Austin, Texas, U.S., 2008, pp. 801–807.

Ayyanar, R., Giri, R. and Mohan, N.. "Active Input–Voltage and Load–Current Sharing in Input–Series and Output–Parallel Connected Modular DC–DC Converters using Dynamic Input–Voltage Reference Scheme." in: IEEE Trans. on Power Electronics, Vol. 19, No. 6, 2004, pp. 1462–1473.

Babasaki, T., Tanaka, T., Nozaki, Y., Tanaka, T., Aoki, T. and Kurokawa, F.. "Developing of Higher Voltage Direct–Current Power–feeding Prototype System." in: Proceedings of the International Telecommunications Energy Conference (INTELEC), Incheon, Korea, 2009.

Badstuebner, U., Biela, J., and Kolar, J.W.. "An Optimized, 99 % Efficient, 5kW, Phase–Shift PWM DC–DC Converter for Data Centers and Telecom Applications." in: Proceedings of the The International Power Electronics Conference (IPEC), Sapporo, Japan, 2010, pp. 626–634.

Eckardt, B., Hofmann, A., Zeltner, S. and Maerz, M.. "Automotive Powertrain DC/DC Converter with 25kW/dm<sup>3</sup> by using SiC Diodes." in: Proceedings of 4th International Conference on Integrated Power Systems (CIPS), Naples, Italy, 2006.

Fan, H. and Li, H.. "A Distributed Control of Input–Series–Output–Parallel Bidirectional DC–DC Converter Modules Applied for 20 kVA Solid State Transformer." In: Proceedings of Twenty–Sixth Applied Power Electronics Conference and Exposition (APEC), Texas, U.S., 2011, pp. 939–945.

Fu, D., Lee, F. C., Liu, Y. and Xu, M.. "Novel Multi–Element Resonant Converters for Front–end DC/DC Converters." Proceedings of 39th IEEE Power Electronics Specialists Conference (PESC2008), 2008, pp. 250–256.

Glaser, J. S. and Witulski, A.F.. "Output Plane Analysis of Load–Sharing in Multiple–Module Converters Systems." in: IEEE Trans. on Power Electronics, Vol. 9, No.1, 1994, pp. 43–50.

Glaser, J. S., Nasadoski, J. and Heinrich, R.. "A 900W, 300V to 50V Dc–dc Power Converter with a 30MHz Switching Frequency." in: Proceedings of Twenty–Fourth Applied Power Electronics Conference and Exposition (APEC), Washington DC, U.S., 2009, pp. 1121–1128.

Gong, Z., Chen, Q., Yang, X., Yuan, B., Feng, W. and Wang, Z.. "Design of High Power Density DC–DC Converter Based on Embedded Passive Substrate." in: Proceedings of 39th IEEE Power Electronics Specialists Conference (PESC2008), Rhodes, Greece, 2008, pp. 273–277.

Hayashi, Y. and Mino, M.. "An Approach to a Higher–Power–Density Power Supply for 380–V DC Distribution System." in: IEEJ Transactions on Industry Applications, Vol.132, No.8, 2012, pp.1–9 (in Japanese).

Hayashi, Y. and Mino, M.. "Series–Parallel Connected 10W/cm<sup>3</sup> Dc–dc Converter for Advanced High–Density Converter Design." in: Proceedings of the International Telecommunications Energy Conference (INTELEC),

Amsterdam, Netherland, 2011.

Hayashi, Y., Takao, K., Shimizu, T. and Ohashi, H. "Power Loss Design Platform for High Output Power Density Converters." in: Proceedings of European Conference on Power Electronics and Application (EPE), pp. 1–10, Aalborg, Denmark, Sep., 2007.

Hayashi, Y. "Multi-converter approach to higher power density DC-DC converter for 380 V DC distribution system." in: Journal of Energy and Power Engineering, JEPE12101601, July 2013 (to be published).

Iyasu, S., Shimizu, T. and Ishii, K. "A Novel Inductor Loss Calculation Method on Power Converters Based on Dynamic Minor Loop." in: IEEJ Transactions on Industry Applications, Volume 126-D Number 7, pp. 1028–1034, 2006.

Kim, J. W., You, J. S. and Cho, B. H. "Modeling, Control, and Design of Input-Series-Output-Parallel-Connected Converter for High-Speed-Train Power System." in: IEEE Trans. on Industrial Electronics, Vol. 48, No. 3, 2001, pp. 536–544.

Kim, K. and Shimizu, T. "Dynamic Iron Loss Measurement Method for an AC Filter Inductor on a PWM Inverter." in: Proceedings of the 12th European Conference on Power Electronics and Applications (EPE) 2007, Aalborg, Denmark, 2007.

Kimball, J. W., Mossoba, J. T. and Krein, P. T. "A Stabilizing, High-Performance Controller for Input Series-Output Parallel Converters." in: IEEE Trans. on Power Electronics, Vol. 23, No. 3, 2008, pp. 1416–1427.

Lee, J. P., Min, B. D., Kim, T. J., Yoo, D. W. and Yoo, J. Y. "High Efficient Interleaved Input-Series-Output-Parallel- Connected DC/DC Converter for Photovoltaic Power Conditioning System." in: Proceedings of Energy Conversion Congress and Exposition (ECCE), California, U.S., 2009, pp. 327–329.

Martinez, C., Jalakas, T., Vinnikov, D., Lazaro, A. and Barrado, A. "QZSI DC/DC Converters in Input-Series Output-Parallel Connection for Distributed Generation." in: Proceedings of International Symposium on Power Electronics, Electrical Drives, Automation and Motion (SPEEDAM), Sorrento, Italia, 2012, pp. 952–957.

Miftakhutdinov, R. "Power Distribution Architecture for Tele- and Data Communication System Based on New Generation Intermediate Bus Converter." in: Proceedings of the 30th International Telecommunications Energy Conference (INTELEC), San Diego, U.S., 2008.

Ninomiya, T., Ishizuka, Y., Shibahara, R. and Abe, S. "Energy-Saving Technology Using Next-Generation Power Electronics." in: Proceedings of the IEE-Japan Industry Applications Society Conference, Chiba, Japan, 2012, pp. I15–I20 (in Japanese).

Noritake, M., Ushirokawa, T., Hirose, K. and Mino, M. "Verification of 380 Vdc Distribution System Availability Based on Demonstration Tests." in: Proceedings of the International Telecommunications Energy Conference (INTELEC), Amsterdam, Netherland, 2011.

Omura, I., Tsukuda, M., Saito, W. and Domon, T. "High Power Density Converter Using SiC-SBD." in: Proceedings of the Fourth Power Conversion Conference PCC Nagoya 2007, Nagoya, Japan, 2007., pp. 575–580.

Pavlovsky, M., Tsuruta, Y., Kawamura, A. "Pursuing High Power-Density and High Efficiency in DC-DC Converters for Automotive Application." in: Proceedings of 39th IEEE Power Electronics Specialists Conference (PESC), Rhodes, Greece, 2008, pp. 4142–4148.

Reusch, D., Gilham, D., Su, Y. and Lee, Fred C. "Gallium Nitride Based 3D Integrated Non-Isolated Point of Load Module." in: Proceedings of Twenty-Seventh Annual IEEE Applied Power Electronics Conference and Exposition (APEC), Florida, U.S., 2012, pp. 38–45.

Schmidt, R. R., Belady, C., Classen, A., Davidson, T., Herrlin, M.K., Novotny, S. and Perry, R. "Evolution of Data Center Environmental Guidelines." in: ASHRAE Transactions, Vol. 110, Part1, 2004, pp. 559–566.

Sun, J., Xu, M., Ying, Y. and Lee, F. C. "High Power Density, High Efficiency System Two-stage Power Architecture for Laptop Computers." in: Proceedings of 37th IEEE Power Electronics Specialists Conference (PESC), Jeju, Korea, 2006, pp. 231–237.

Takao, K., Irokawa, H., Hayashi, Y. and Ohashi, H. "Novel exact power loss design method for high output power density converter." in: Proceedings of 37th IEEE Power Electronics Specialists Conference (PESC), pp. 2651–2655, Jeju, Korea, 2006.

Wang, L. and He, X. "Input-Series and Output-Parallel Connection Modular DC-DC Converters with Interleaved

Constant Duty Cycle Control Strategy." in: Proceedings of the 33rd Annual Conference of the IEEE Industrial Electronics Society (IECON), Taipei, Taiwan, 2007, pp. 1901–1906.

Wang, Y., de Haan, S. W. H. and Ferreira, J. A.. "Potential of improving PWM converter power density with advanced components." in: Proceedings of the 13th European Conference on Power Electronics and Applications (EPE) 2009, Barcelona, Spain, 2009.



**Yusuke Hayashi** completed a postdoctoral course in engineering at Osaka University Graduate School in 2004. In April 2004, he joined the AIST Power Electronics Research Center, in April 2009 he joined NTT Facilities, and since May 2013 he has been with Osaka University. He is engaged in the research and development of the power quality control in the distribution system, and the development of the design methodology for high power density converter using SiC and GaN power devices. Currently, he is mainly engaged in the development of the high power density DC power supply for 380 V DC distribution system.